Quantum Thermodynamics of Nonequilibrium Processes in Lattice Gauge Theories

Zohreh Davoudi,[1,2,3,4,*] Christopher Jarzynski,[5,6,1,4,†] Niklas Mueller,[7,‡] Greeshma Oruganti,[6,4,§] Connor Powers,[1,2,3,4,‖] and Nicole Yunger Halpern[3,6,4,¶]

[1]*Department of Physics, University of Maryland, College Park, Maryland 20742 USA*
[2]*Maryland Center for Fundamental Physics, University of Maryland, College Park, Maryland 20742, USA*
[3]*Joint Center for Quantum Information and Computer Science, NIST and University of Maryland, College Park, Maryland 20742 USA*
[4]*The NSF Institute for Robust Quantum Simulation, University of Maryland, College Park, Maryland 20742, USA*
[5]*Department of Chemistry and Biochemistry, University of Maryland, College Park, Maryland 20742 USA*
[6]*Institute for Physical Science and Technology, University of Maryland, College Park, Maryland 20742, USA*
[7]*InQubator for Quantum Simulation (IQuS), Department of Physics, University of Washington, Seattle, Washington 98195, USA*

(Received 3 June 2024; revised 15 August 2024; accepted 3 September 2024; published 19 December 2024)

A key objective in nuclear and high-energy physics is to describe nonequilibrium dynamics of matter, e.g., in the early Universe and in particle colliders, starting from the standard model of particle physics. Classical computing methods, via the framework of lattice gauge theory, have experienced limited success in this mission. Quantum simulation of lattice gauge theories holds promise for overcoming computational limitations. Because of local constraints (Gauss's laws), lattice gauge theories have an intricate Hilbert-space structure. This structure complicates the definition of thermodynamic properties of systems coupled to reservoirs during equilibrium and nonequilibrium processes. We show how to define thermodynamic quantities such as work and heat using strong-coupling thermodynamics, a framework that has recently burgeoned within the field of quantum thermodynamics. Our definitions suit instantaneous quenches, simple nonequilibrium processes undertaken in quantum simulators. To illustrate our framework, we compute the work and heat exchanged during a quench in a $\mathbb{Z}_2$ lattice gauge theory coupled to matter in $1+1$ dimensions. The thermodynamic quantities, as functions of the quench parameter, evidence a phase transition. For general thermal states, we derive a simple relation between a quantum many-body system's entanglement Hamiltonian, measurable with quantum-information-processing tools, and the Hamiltonian of mean force, used to define strong-coupling thermodynamic quantities.

DOI: 10.1103/PhysRevLett.133.250402

Introduction—An overarching goal in nuclear and high-energy physics is to simulate strongly interacting matter, starting from gauge theories. Key focuses include nonequilibrium phenomena described by quantum chromodynamics (QCD), the theory of the strong force. Nonequilibrium phenomena arise in ultrarelativistic particle collisions [1,2] and in the early Universe [3,4]. Theoretical studies [5–9] of in- and out-of-equilibrium phases of QCD, and of its thermalization mechanisms, are often restricted to extreme parameter regimes to facilitate perturbation theory. Alternatively, studies feature simple (often low-dimensional) models to capture qualitative features of QCD.

Studying QCD and other strongly interacting gauge theories requires nonperturbative tools, as enabled by lattice gauge theory (LGT) [10–14]. Within the path-integral formulation of LGTs, Monte Carlo simulations can be feasible if Euclidean (imaginary) time replaces Minkowski (real) time. The scheme permits parallels with statistical mechanics: Euclidean time stands in for inverse temperature, and vacuum expectation values serve as thermal averages. LGT has enabled thermodynamic studies of the QCD equation of state at small chemical potentials [15–26]. Nonetheless, the sampling weight in Monte Carlo computations can become nonreal, requiring infeasibly many samples [26–30]. These limitations do not inhibit Hamiltonian-based approaches, such as tensor-network methods [31–33] and quantum simulation [34–39]. These approaches, hence, suit thermodynamic studies of gauge theories, in and out of equilibrium. Still, we need a modern description of LGTs in the language of quantum thermodynamics.

The field of quantum thermodynamics extends conventional thermodynamics to small and quantum systems that exchange heat and work [40–42]. A typical setup features a subsystem of interest (the "system") interacting with a "reservoir" of inaccessible degrees of freedom (d.o.f.)

*Contact author: davoudi@umd.edu
†Contact author: cjarzyns@umd.edu
‡Contact author: niklasmu@uw.edu
§Contact author: gshivali@umd.edu
‖Contact author: cdpowers@umd.edu
¶Contact author: nicoleyh@umd.edu

[43,44]. The coupling is often weak because a system and reservoir typically interact only at their shared boundary. This boundary is of lower dimensionality than the system, whose volume is proportional to its internal energy. Hence, the interaction energy is much smaller than the system's and reservoir's internal energies. Yet quantum systems and reservoirs can be small while behaving thermodynamically [45–47]; their interactions need not be negligible.

Hence, the subfield of strong-coupling (quantum) thermodynamics has burgeoned recently [48–57]. Strong coupling blurs the system-reservoir boundary, complicating the definition of the system's internal energy, work, and heat. Nonetheless, definitions have been developed and obey thermodynamic laws [52,54,55,58–60].

These considerations raise the question of whether *weak-coupling thermodynamics can describe LGTs*. Local constraints, or Gauss's laws, form the defining feature of (lattice) gauge theories: the charge at a site balances the electric-field flux emanating from the site. Only a subspace of the gauge theory's Hilbert space satisfies Gauss's laws and consists of physical states. This restriction complicates the partitioning of the system into subsystems: the values of the fields on one side of any partition depend on the values on the other side. Yet a partitioning is used to define quantities such as the bipartite entanglement entropy [61–68]. The system-reservoir partitioning in LGTs, we posit, can resemble that in strong-coupling thermodynamics. Hence, we use strong-coupling thermodynamics to define thermodynamic properties of LGTs.

We answer the following questions: What are the work and heat exchanged during instantaneous quenches [69] (simple nonequilibrium processes created in quantum simulations) [70,71]? Can these quantities signal phase transitions [72]? Can such quantities be measured efficiently with quantum-information-processing tools?

We describe how to compute internal-energy changes. We further show how to define work and heat consistently with the first and second laws of thermodynamics [58]. A simple model illustrates this framework: a $\mathbb{Z}_2$ LGT coupled to hardcore bosonic matter in $1+1$ dimensions (D). We observe that thermodynamic quantities, as functions of chemical potential, signal an apparent phase transition. Furthermore, we bridge the fields of quantum information theory and strong-coupling quantum thermodynamics: we show that the entanglement Hamiltonian [81,82], which can often be efficiently measured experimentally [83–86], is related to the Hamiltonian of mean force [52], which underpins strong-coupling quantum thermodynamics.

Review of strong-coupling quantum thermodynamics—Consider a system S and a reservoir R. The composite $S \cup R$ evolves under the Hamiltonian

$$H_{S\cup R} \coloneqq H_S + H_R + V_{S\cup R}. \tag{1}$$

H_S and H_R denote the system and reservoir Hamiltonians, respectively; $V_{S\cup R}$ denotes the interaction. During a thermodynamic process, S can absorb heat Q and work W. (*Heat*, *work*, and *internal energy* refer to averages throughout this Letter.)

In weak-coupling quantum thermodynamics, $V_{S\cup R}$ contributes negligibly to the total internal energy, $U_{S\cup R} \coloneqq \langle H_{S\cup R}\rangle$. Hence, the system's internal energy is $U_S \coloneqq \langle H_S\rangle$ [59]. One can measure U_S by accessing only system d.o.f. In contrast, when $\langle V_{S\cup R}\rangle$ is comparable to $\langle H_S\rangle$, one must use strong-coupling thermodynamics.

How much $V_{S\cup R}$ contributes to U_S is ambiguous. To resolve the ambiguity, one can define the global Gibbs state with respect to an inverse temperature β: $\pi_{S\cup R} \coloneqq e^{-\beta H_{S\cup R}}/Z_{S\cup R}$. The partition function is $Z_{S\cup R} \coloneqq \mathrm{Tr}(e^{-\beta H_{S\cup R}})$. Throughout this Letter, we denote thermal states by π and general density matrices by ρ. Tr_X denotes the partial trace over X. Consider tracing out the reservoir from $\pi_{S\cup R}$. The system's reduced density matrix is $\pi_S \coloneqq \mathrm{Tr}_R(\pi_{S\cup R}) \equiv e^{-\beta H_S^*}/Z_S^*$. This is a thermal state with respect to an effective Hamiltonian, a "Hamiltonian of mean force" [52],

$$H_S^* \coloneqq -\frac{1}{\beta}\ln\left(\frac{\mathrm{Tr}_R(e^{-\beta H_{S\cup R}})}{Z_R}\right), \tag{2}$$

wherein $Z_R \coloneqq \mathrm{Tr}_R(e^{-\beta H_R})$ and $Z_S^* \coloneqq \mathrm{Tr}_S(e^{-\beta H_S^*}) = Z_{S\cup R}/Z_R$. Equation (2) underlies an intuitive definition for the system's free energy [52,87,88],

$$F_S \coloneqq -\frac{1}{\beta}\ln(Z_S^*). \tag{3}$$

It is natural to equate $\langle H_S^*\rangle$ with U_S [51,58,59,87]. Consequently, once H_S^* has been determined by tracing over the reservoir d.o.f. [Eq. (2)], one need not access reservoir d.o.f. further to compute U_S. Furthermore, if $\mathcal{S} \coloneqq -\mathrm{Tr}_S(\pi_S \ln \pi_S)$ denotes the thermal von Neumann entropy, then the equality $F_S = U_S - \frac{\mathcal{S}}{\beta}$ holds in equilibrium [89].

Any change in U_S comes from work and heat, by the first law of thermodynamics: $\Delta U_S = W + Q$. By the second law, $\Delta F_S \leq W$, or $Q \leq \Delta\mathcal{S}/\beta$. Here, ΔU_S, ΔF_S, and $\Delta\mathcal{S}$ denote, respectively, net changes in the system's internal energy, free energy, and entropy. Intuition guides the separation of ΔU_S into W and Q: work comes from changes in the system's Hamiltonian and heat from changes in the system's state [41]. To define work and heat, we now specify a thermodynamic process.

Instantaneous quenches—During a quench, the Hamiltonian changes rapidly. Quenches generate nonequilibrium conditions and are studied in diverse quantum-simulation experiments [86,90–100]. Figure 1 depicts the quench studied here. The system-reservoir composite begins in a Gibbs state: $\rho_{S\cup R}^{\mathrm{i}} \coloneqq \rho_{S\cup R}(t=0^-) = \pi_{S\cup R}^{\mathrm{i}} \coloneqq e^{-\beta H_{S\cup R}^{\mathrm{i}}}/\mathrm{Tr}(e^{-\beta H_{S\cup R}^{\mathrm{i}}})$, wherein the initial composite Hamiltonian $H_{S\cup R}^{\mathrm{i}} \coloneqq H_{S\cup R}(t=0^-)$. Equation (1), with a time-dependent $H_S(t)$, specifies $H_{S\cup R}$. At time $t=0$, $H_S(t)$ is instantaneously quenched from $H_S(t=0^-) \coloneqq H_S^{\mathrm{i}}$ to $H_S(t=0^+) \coloneqq H_S^{\mathrm{f}}$. The system-reservoir composite

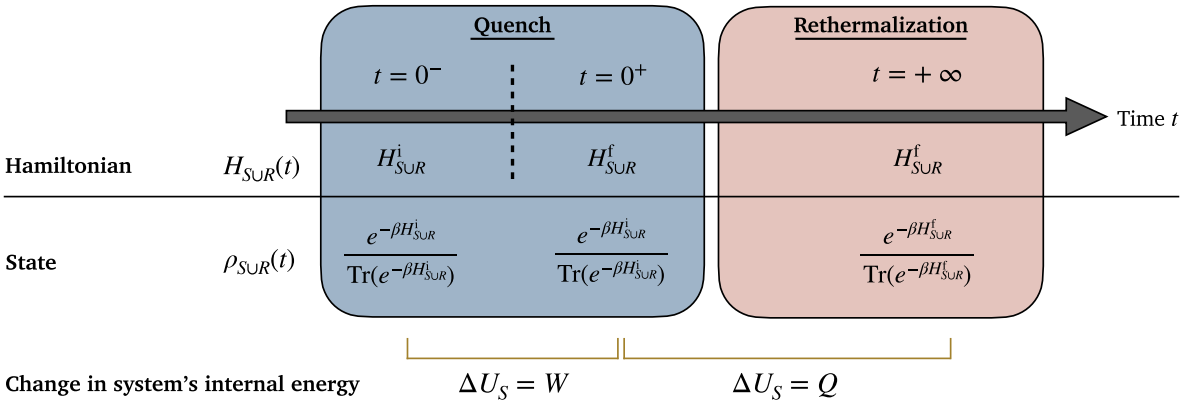

FIG. 1. Overview of relevant quench protocol. The system starts in a global Gibbs state. At $t = 0$, the system Hamiltonian H_S is quenched instantaneously. Under the new total Hamiltonian, the system-reservoir composite equilibrates to a global Gibbs state with the initial state's temperature.

equilibrates to a Gibbs state under the final total Hamiltonian $H_{S\cup R}(t = 0^+) \coloneqq H^{\mathrm{f}}_{S\cup R}$. The initial and final Gibbs states share the temperature β^{-1} by assumption. Justifications include the possibility that $S \cup R$ couples weakly to a larger reservoir, at a temperature β^{-1}, in the distant past and future [58].

Practical work and heat definitions depend on system d.o.f. alone. We present such definitions, for the quenches just described, in Ref. [58]; see also Refs. [49,52,87]. The system's internal energy is

$$U_S(t) \coloneqq \langle H^*_S(t)\rangle = \mathrm{Tr}[\rho_S(t)H^*_S(t)], \tag{4}$$

for arbitrary states $\rho_S(t) \coloneqq \mathrm{Tr}_R[\rho_{S\cup R}(t)]$. H^*_S becomes time-dependent under the replacement $\mathrm{Tr}_R(e^{-\beta H_{S\cup R}}) \mapsto \mathrm{Tr}_R(e^{-\beta H_{S\cup R}(t)})$ in Eq. (2). During the quench, ΔU_S equals the work absorbed by S:

$$W \coloneqq \mathrm{Tr}_S[\rho^{\mathrm{i}}_S H^*_S(t = 0^+)] - \mathrm{Tr}_S[\rho^{\mathrm{i}}_S H^*_S(t = 0^-)]. \tag{5}$$

During the equilibration, ΔU_S equals the heat absorbed by S:

$$Q \coloneqq \mathrm{Tr}_S[\rho^{\mathrm{f}}_S H^*_S(t = 0^+)] - \mathrm{Tr}_S[\rho^{\mathrm{i}}_S H^*_S(t = 0^+)]. \tag{6}$$

These definitions are intuitive and obey the first and second laws of thermodynamics [58]. Upon identifying a Hamiltonian of the form in Eq. (1), one calculates work and heat by measuring $\langle H^*_S\rangle$. We show next how to measure this quantity.

Measuring thermodynamic quantities in quantum simulations—Here, we derive a relation between strong-coupling-thermodynamics quantities and a quantity called the "entanglement Hamiltonian." Every density matrix ρ can be expressed as $\rho = \sum_k p_k|k\rangle\langle k|$. The $|k\rangle$ denote eigenstates and the $p_k \in [0, 1]$, probabilities. Define $\lambda_k \coloneqq -\ln(p_k) \geq 0$, such that $\rho = \sum_k e^{-\lambda_k}|k\rangle\langle k|$. This expansion has the form of a thermal state at unit temperature (with the normalization factor, or partition function, absorbed into the $e^{-\lambda_k}$). For $\rho = \rho_S \coloneqq \mathrm{Tr}_R(\rho_{S\cup R})$, this Hamiltonian is the "(bipartite) entanglement Hamiltonian" [81,82],

$$H^{\mathrm{ent}}_S \coloneqq -\ln(\rho_S). \tag{7}$$

This operator contains more information than the bipartite entanglement entropy. It has spawned numerous studies in quantum information theory and many-body physics. Parametrized *Ansätze* for entanglement Hamiltonians [82], with random-measurement protocols [101–104], enable tomography of ground and nonequilibrium states [83–85,105,106], including of LGTs [86,107,108].

To leverage such tomography tools, we prove a relation between H^{ent}_S and H^*_S for thermal states. We rewrite the Hamiltonian of mean force as

$$H^*_S = -\frac{1}{\beta}\ln\left(\frac{\mathrm{Tr}_R(e^{-\beta H_{S\cup R}})}{\mathrm{Tr}_R(e^{-\beta H_R})}\right) \tag{8a}$$

$$= -\frac{1}{\beta}\ln\left(\rho_S\frac{Z_{S\cup R}}{Z_R}\right). \tag{8b}$$

The system's reduced state is $\rho_S = \pi_S \coloneqq \mathrm{Tr}_R(e^{-\beta H_{S\cup R}})/Z_{S\cup R}$. Using Eqs. (7) and (3) yields the relation between the entanglement Hamiltonian and the Hamiltonian of mean force:

$$H^*_S = \frac{1}{\beta}H^{\mathrm{ent}}_S + F_S. \tag{9}$$

$\mathbb{I}_S$ denotes the identity operator defined on S.

One can measure the first term in Eq. (9) using the aforementioned tomography tools (if the *Ansätze* model H^{ent}_S accurately). To measure F_S, one must measure $Z_{S\cup R}$ and Z_R [109–112], necessitating access to the reservoir

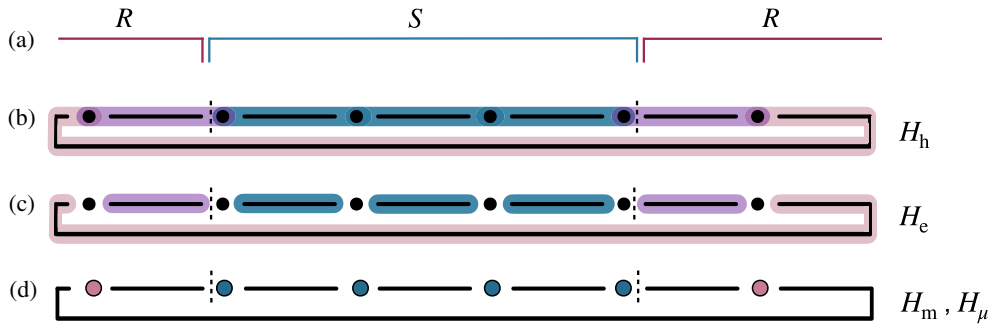

FIG. 2. (a) Partitioning of d.o.f. into system (S) and reservoir (R) d.o.f. Partitioning of total Hamiltonian's (b) hopping terms, (c) electric-field terms, and (d) mass and chemical-potential terms into $H_S(t)$ (teal), H_R (light red), and $V_{S\cup R}$ (purple). Matter (gauge-field) d.o.f. reside on lattice sites (links). The last link wraps around to indicate the lattice's periodicity.

d.o.f. To avoid measuring the second term in Eq. (9), we study the average dissipated work, $W_{\mathrm{diss}} \coloneqq W - \Delta F_S$, a measure of entropy production [113,114]. For our quench protocol,

$$W_{\mathrm{diss}} = \frac{1}{\beta}\mathrm{Tr}_S\{\rho_S^{\mathrm{i}}[H_S^{\mathrm{ent}}(t=0^+) - H_S^{\mathrm{ent}}(t=0^-)]\}. \tag{10}$$

Hence, one can infer W_{diss} upon measuring the entanglement Hamiltonian alone.

Lattice gauge theories and strong-coupling quantum thermodynamics—We use the Hamiltonian formulation of LGTs [12], which suits quantum simulation. As matter and gauge fields undergo local symmetry-group transformations, the observables remain invariant. The symmetry restricts the states to a "physical subspace": for each site n, a "Gauss-law" operator G_n acts on n and commutes with the Hamiltonian. The full Hilbert space (spanned by eigenbases of electric and matter fields) decomposes into G_n eigenspaces, for each n. The eigenspace labeled by some eigenvalue g, and shared by all the G_n, is the physical subspace [115]. That is, for any physical state $|\Psi_{\mathrm{phys}}\rangle$,

$$G_n|\Psi_{\mathrm{phys}}\rangle = g|\Psi_{\mathrm{phys}}\rangle, \quad \forall\ n. \tag{11}$$

In electrodynamics, $G_n = \boldsymbol{\nabla}\cdot\boldsymbol{E}_n - \rho_n$. Here, $\boldsymbol{E}_n$ denotes the electric field, and ρ_n denotes the (dynamical) electric-charge density, both at site n. Gauss's law follows from setting $g = 0$ ($g \neq 0$) in Eq. (11) in the absence (presence) of a background static electric charge.

One may impose Gauss's laws by manually removing the unphysical states from the full Hilbert space [116,117]. Alternatively, the Hamiltonian $H_{S\cup R}$ may be replaced with $H_{S\cup R} + \sum_n f(G_n)$. $f(G_n)$ denotes a function of Gauss-law operators. Chosen properly, it penalizes transitions to unphysical states [118–125]. Consider partitioning a lattice into a system S and a reservoir R. Some Gauss-law penalty terms act on both S and R: Gauss-law operators are multibody operators consisting of gauge and matter fields. Such penalty terms, thus, contribute to the $V_{S\cup R}$ in Eq. (1). Their contribution must be large to constrain the state to the physical subspace. Therefore, one cannot generally neglect the internal energy's dependence on $V_{S\cup R}$ when computing thermodynamic quantities [see Supplemental Material (SM) [126]]. Consequently, LGTs can be described within the framework of strong-coupling thermodynamics.

Example of $\mathbb{Z}_2$ LGT coupled to matter in $(1+1)D$—Consider a $\mathbb{Z}_2$ gauge field (hardcore bosons) coupled to matter fields (chosen to be hardcore bosons). The initial state evolves under the Hamiltonian

$$\begin{aligned} H &= H_{\mathrm{h}} + H_{\mathrm{e}} + H_{\mathrm{m}} + H_{\mu} + H_c \\ &\equiv -J\sum_{n=0}^{N-1}(\sigma_n^+\tilde{\sigma}_n^z\sigma_{n+1}^- + \mathrm{H.c.}) - \epsilon\sum_{n=0}^{N-1}\tilde{\sigma}_n^x \\ &\quad + m\sum_{n=0}^{N-1}(-1)^n\sigma_n^+\sigma_n^- - \sum_{n=0}^{N-1}\mu_n\sigma_n^+\sigma_n^- + c\sum_{n=0}^{N-1}\mathbb{I}_n, \end{aligned} \tag{12}$$

on a one-dimensional N-site spatial lattice with periodic boundary conditions ($\sigma_N = \sigma_0$). H_{h}, H_{e}, H_{m}, and H_{μ} represent the matter-hopping, electric-field, matter-mass, and matter-chemical-potential terms, respectively. A constant H_c is added such that $H_S(t)$, H_R, and $H_{S\cup R}(t)$ have only non-negative eigenvalues. J, ϵ, m, and μ_n denote the hopping strength, electric-field strength, matter mass, and site-n chemical potential, respectively. Pauli operator σ_n acts on the Hilbert space of the site-n matter field. Pauli operator $\tilde{\sigma}_n$ acts on the Hilbert space of the gauge field rightward of n. Specifically, $\tilde{\sigma}_n^x$ ($\tilde{\sigma}_n^z$) denotes the electric-field (gauge-link) operator.

The $\mathbb{Z}_2$ gauge transformation is generated by the Gauss-law operator [128]

$$G_n = \tilde{\sigma}_n^x\tilde{\sigma}_{n-1}^x \exp\left(i\pi\left[\sigma_n^+\sigma_n^- + \frac{(-1)^n - 1}{2}\right]\right). \tag{13}$$

The physical states obey Eq. (11) with $g = 1$. One can realize the gauge-invariant dynamics by adding $\sum_n f(G_n) = \kappa\sum_n(1 - G_n)$ to H, then taking the limit $\kappa \to \infty$ [129].

The lattice can be partitioned into a system S and a reservoir R, as in Fig. 2(a). Also, the Hamiltonian (12) decomposes as in Eq. (1). Some hopping terms act only on sites in S (R) and so belong in H_S (H_R). Other terms

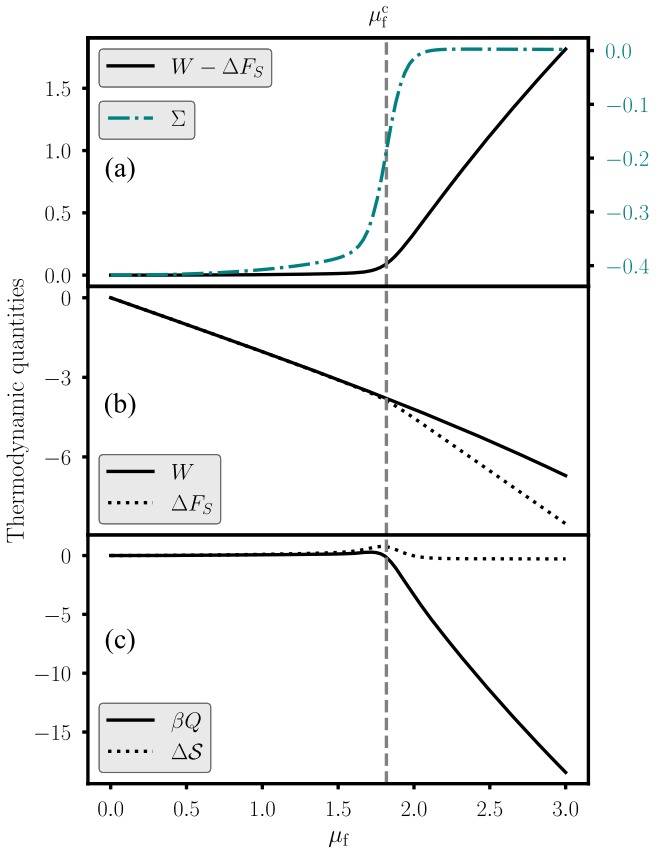

FIG. 3. Thermodynamic quantities as functions of the final chemical potential, μ_f, during the instantaneous quench from $\mu_i = 0$ with $N = 6$, $N_S = 4$, $t = -1/2$, $\epsilon = 1/2$, $m = 1/2$, $\mu_i = 0$, and $\beta = 10$. (a) Dissipated work W_{diss} (solid, black) and chiral condensate Σ (dot-dashed, teal). (b) Work W (solid, black) and change ΔF_S in the system's free energy (dotted, black). (c) Normalized heat βQ (solid, black) and change $\Delta \mathcal{S}$ in the system's entropy (dotted, black). We also plot μ_f^c, the μ_f value where Σ' is maximized (dashed, gray).

describe hopping between a site in S and a site in R. These interaction terms belong in $V_{S\cup R}$; see Fig. 2(b). The electric-field Hamiltonian can be partitioned as follows; see Fig. 2(c). Terms acting on links in S belong in $H_S(t)$. Terms acting on links in R, but touching the S-R boundary, belong in $V_{S\cup R}$ due to Gauss's laws. Terms acting on links elsewhere in R belong in H_R. Terms in H_m and H_μ belong in $H_S(t)$ and H_R, depending on whether they act on a site in S or R; see Fig. 2(d). Finally, if penalty terms enforcing Gauss's law act at the boundary, they belong in $V_{S\cup R}$. Otherwise, they belong in H_S or H_R.

We set reservoir's chemical potential to zero and quench the chemical potential from $\mu_n = \mu_i = 0$ to $\mu_n = \mu_f > 0$ at all sites n in the system. We further define the "chiral condensate" [130]

$$\Sigma \coloneqq \frac{1}{N_S} \sum_{n=0}^{N_S-1} (-1)^n \langle \sigma_n^+ \sigma_n^- \rangle. \tag{14}$$

N_S denotes the system size. The expectation value is in the final thermal state, whose $\mu_n = \mu_f$ at all sites n in S. If $\mu_f \gg \epsilon$, m, the system's state is dominated by the matter fields' all-spin-up state, yielding $\Sigma = 0$. At other μ_f values, Σ could be nonvanishing. In fact, Σ suddenly changes from finite to vanishing values as μ_f increases, evidencing a phase transition, as Fig. 3(a) shows. This apparent phase transition does not look perfectly sharp due to finite-temperature (see SM [126]) and finite-size effects [131]. The critical value $\mu_f = \mu_f^c$ denotes the transition point, where $\Sigma' \coloneqq d\Sigma/d\mu_f$ is maximized.

Figure 3 displays thermodynamic quantities, W_{diss}, W, Q, ΔF_S, and $\Delta \mathcal{S}$, calculated as functions of μ_f. As μ_f grows, $W_{\text{diss}} \coloneqq W - \Delta F_S$ remains near zero until around the μ_f value where the apparent phase transition occurs. Afterward, W_{diss} increases. Hence, W_{diss} indicates the suspected phase transition clearly. Similarly, W (βQ) begins deviating from ΔF_S ($\Delta \mathcal{S}$) around the transition.

Strong-coupling relations are valid in this model: $|\langle V_{S\cup R}\rangle / \langle H_S \rangle|$ is non-negligible ($\gtrsim 0.1$) in the initial and final states at all the μ_f values used. Nonetheless, in the SM [126], we apply weak-coupling relations for comparison: $U_S = \langle H_S \rangle$ and $\rho_S = e^{-\beta H_S}/\text{Tr}(e^{-\beta H_S})$. We find that the thermodynamic quantities' values differ from their strong-coupling counterparts: the weak-coupling quantities change less sharply, signaling the transition less reliably.

Outlook—This work shows how strong-coupling quantum thermodynamics applies to lattice gauge theories in and out of equilibrium. The work further shows how entanglement Hamiltonians can be leveraged to measure thermodynamic quantities in quantum simulations. Our framework may be applied to explore further questions in the quantum thermodynamics of gauge theories. Examples include whether thermodynamic quantities signal topological [81,134–141] or dynamical [142] phase transitions. While quench protocols in LGTs have been implemented in experiments [86,96–98,100,119,143–153], a longer-term vision is to simulate more-general processes, including quantum-adiabatic ones, and particle collisions relevant to nuclear and high-energy physics [154–159]. Also, non-Abelian and higher-dimensional gauge theories merit studying within our framework. Developing quantum-simulation protocols for studying gauge-theory thermodynamics is an active frontier, and this work furthers this goal.

Acknowledgments—Z. D., G. O., and C. P. were supported by the National Science Foundation (NSF) Quantum Leap Challenge Institutes (QLCI) (Award No. OMA-2120757). Z. D. further acknowledges funding by the Department of Energy (DOE), Office of Science, Early Career Award (Award No. DESC0020271), and by the Department of Physics, Maryland Center for Fundamental Physics, and the College of Computer, Mathematical, and Natural Sciences at the University of Maryland, College Park. She is grateful for the hospitality

of Perimeter Institute where part of this work was carried out. Research at Perimeter Institute is supported in part by the Government of Canada through the Department of Innovation, Science, and Economic Development, and by the Province of Ontario through the Ministry of Colleges and Universities. Z. D. was also supported in part by the Simons Foundation through the Simons Foundation Emmy Noether Fellows Program at Perimeter Institute. C. J. and N. Y. H. further acknowledge support from John Templeton Foundation (Award No. 62422). N. Y. H. thanks Harry Miller for conversations about strong-coupling thermodynamics. N. M. acknowledges funding by the DOE, Office of Science, Office of Nuclear Physics, Inqubator for Quantum Simulation (Award No. DE-SC0020970). C. P. is grateful for discussions on thermal gauge theories with Robert Pisarski, and for the hospitality of Brookhaven National Laboratory, which hosted C. P. as part of an Office of Science Graduate Student Research Fellowship. G. O. further acknowledges support from the American Association of University Women through an International Fellowship. Finally, N. M., G. O., C. P., and N. Y. H. thank the participants of the InQubator for Quantum Simulation (IQuS) workshop "Thermalization, from Cold Atoms to Hot Quantum Chromodynamics" at the University of Washington in September 2023 for many valuable discussions.

[1] R. Vogt, *Ultrarelativistic Heavy-Ion Collisions* (Elsevier, New York, 2007).
[2] W. Florkowski, *Phenomenology of Ultra-Relativistic Heavy-Ion Collisions* (World Scientific Publishing Company, Singapore, 2010).
[3] P. J. E. Peebles, *Principles of Physical Cosmology* (Princeton University Press, Princeton, NJ, 1993).
[4] E. Kolb, *The Early Universe* (CRC Press, Boca Raton, Florida, 2018).
[5] J. B. Kogut and M. A. Stephanov, *The Phases of Quantum Chromodynamics: From Confinement to Extreme Environments* (Cambridge University Press, Cambridge, England, 2003).
[6] J. Ghiglieri, A. Kurkela, M. Strickland, and A. Vuorinen, Perturbative thermal QCD: Formalism and applications, Phys. Rep. **880**, 1 (2020).
[7] J. Berges, M. P. Heller, A. Mazeliauskas, and R. Venugopalan, QCD thermalization: *Ab initio* approaches and interdisciplinary connections, Rev. Mod. Phys. **93**, 035003 (2021).
[8] A. Lovato *et al.*, Long range plan: Dense matter theory for heavy-ion collisions and neutron stars, arXiv:2211.02224.
[9] P. Achenbach *et al.*, The Present and Future of QCD, Nucl. Phys. **A1047**, 122874 (2024).
[10] K. G. Wilson, Confinement of quarks, Phys. Rev. D **10**, 2445 (1974).
[11] J. Kogut and L. Susskind, Hamiltonian formulation of Wilson's lattice gauge theories, Phys. Rev. D **11**, 395 (1975).
[12] J. B. Kogut, An introduction to lattice gauge theory and spin systems, Rev. Mod. Phys. **51**, 659 (1979).
[13] M. Creutz, *Quarks, Gluons and Lattices* (Cambridge University Press, Cambridge, England, 1983).
[14] M. Creutz, L. Jacobs, and C. Rebbi, Monte Carlo computations in lattice gauge theories, Phys. Rep. **95**, 201 (1983).
[15] Y. Aoki, G. Endrődi, Z. Fodor, S. D. Katz, and K. K. Szabó, The order of the quantum chromodynamics transition predicted by the standard model of particle physics, Nature (London) **443**, 675 (2006).
[16] Y. Aoki, Z. Fodor, S. Katz, and K. K. Szabó, The QCD transition temperature: Results with physical masses in the continuum limit, Phys. Lett. B **643**, 46 (2006).
[17] Y. Aoki *et al.*, The QCD transition temperature: Results with physical masses in the continuum limit II, J. High Energy Phys. 06 (2009) 088.
[18] S. Borsányi *et al.*, Is there still any T c mystery in lattice QCD? Results with physical masses in the continuum limit III, J. High Energy Phys. 09 (2010) 73.
[19] T. Bhattacharya *et al.*, QCD phase transition with chiral quarks and physical quark masses, Phys. Rev. Lett. **113**, 082001 (2014).
[20] A. Bazavov *et al.*, Chiral and deconfinement aspects of the QCD transition, Phys. Rev. D **85**, 054503 (2012).
[21] H.-T. Ding, F. Karsch, and S. Mukherjee, Thermodynamics of strong-interaction matter from lattice QCD, Int. J. Mod. Phys. E **24**, 1530007 (2015).
[22] C. Ratti, Lattice QCD and heavy ion collisions: A review of recent progress, Rep. Prog. Phys. **81**, 084301 (2018).
[23] USQCD Collaboration, A. Bazavov, F. Karsch, S. Mukherjee, and P. Petreczky, Hot-dense lattice QCD, Eur. Phys. J. A **55**, 194 (2019).
[24] O. Philipsen, Constraining the QCD phase diagram at finite temperature and density, arXiv:1912.04827.
[25] J. N. Guenther, Overview of the QCD phase diagram, Eur. Phys. J. A **57**, 136 (2021).
[26] K. Nagata, Finite-density lattice QCD and sign problem: Current status and open problems, Prog. Part. Nucl. Phys. **127**, 103991 (2022).
[27] M. Troyer and U.-J. Wiese, Computational complexity and fundamental limitations to fermionic quantum Monte Carlo simulations, Phys. Rev. Lett. **94**, 170201 (2005).
[28] C. Gattringer and K. Langfeld, Approaches to the sign problem in lattice field theory, Int. J. Mod. Phys. A **31**, 1643007 (2016).
[29] A. Alexandru, G. Başar, P. F. Bedaque, and N. C. Warrington, Complex paths around the sign problem, Rev. Mod. Phys. **94**, 015006 (2022).
[30] G. Pan and Z. Y. Meng, Sign Problem in Quantum Monte Carlo Simulation, arXiv:2204.08777.
[31] M. C. Bañuls, K. Cichy, J. I. Cirac, K. Jansen, and S. Kühn, Tensor networks and their use for lattice gauge theories, arXiv:1810.12838.
[32] M. C. Banuls and K. Cichy, Review on novel methods for lattice gauge theories, Rep. Prog. Phys. **83**, 024401 (2020).
[33] Y. Meurice, R. Sakai, and J. Unmuth-Yockey, Tensor lattice field theory for renormalization and quantum computing, Rev. Mod. Phys. **94**, 025005 (2022).

[34] M. C. Bañuls *et al.*, Simulating lattice gauge theories within quantum technologies, Eur. Phys. J. D **74**, 165 (2020).
[35] N. Klco, A. Roggero, and M. J. Savage, Standard model physics and the digital quantum revolution: Thoughts about the interface, Rep. Prog. Phys. **85**, 064301 (2022).
[36] C. W. Bauer *et al.*, Quantum simulation for high-energy physics, PRX Quantum **4**, 027001 (2023).
[37] C. W. Bauer, Z. Davoudi, N. Klco, and M. J. Savage, Quantum simulation of fundamental particles and forces, Nat. Rev. Phys. **5**, 420 (2023).
[38] A. Di Meglio *et al.*, Quantum computing for high-energy physics: state of the art and challenges, PRX Quantum **5**, 037001 (2024).
[39] J. C. Halimeh, M. Aidelsburger, F. Grusdt, P. Hauke, and B. Yang, Cold-atom quantum simulators of gauge theories, arXiv:2310.12201.
[40] J. Goold, M. Huber, A. Riera, L. del Rio, and P. Skrzypczyk, The role of quantum information in thermodynamics—a topical review, J. Phys. A **49**, 143001 (2016).
[41] S. Vinjanampathy and J. Anders, Quantum thermodynamics, Contemp. Phys. **57**, 545 (2016).
[42] N. Yunger Halpern, *Quantum Steampunk: The Physics of Yesterday's Tomorrow* (JHU Press, Baltimore, 2022).
[43] H.-P. Breuer and F. Petruccione, *The Theory of Open Quantum Systems* (Oxford University Press, Oxford, 2007).
[44] S. Deffner and S. Campbell, The principles of modern thermodynamics, in *Quantum Thermodynamics* (Morgan & Claypool Publishers, San Rafael, 2019), pp. 1–1 to 2–37.
[45] L. D'Alessio, Y. Kafri, A. Polkovnikov, and M. Rigol, From quantum chaos and eigenstate thermalization to statistical mechanics and thermodynamics, Adv. Phys. **65**, 239 (2016).
[46] A. M. Kaufman, M. E. Tai, A. Lukin, M. Rispoli, R. Schittko, P. M. Preiss, and M. Greiner, Quantum thermalization through entanglement in an isolated many-body system, Science **353**, 794 (2016).
[47] A. Polkovnikov and D. Sels, Thermalization in small quantum systems, Science **353**, 752 (2016).
[48] F. Binder, S. Vinjanampathy, K. Modi, and J. Goold, Quantum thermodynamics of general quantum processes, Phys. Rev. E **91**, 032119 (2015).
[49] U. Seifert, First and second law of thermodynamics at strong coupling, Phys. Rev. Lett. **116**, 020601 (2016).
[50] P. Strasberg, G. Schaller, N. Lambert, and T. Brandes, Nonequilibrium thermodynamics in the strong coupling and non-Markovian regime based on a reaction coordinate mapping, New J. Phys. **18**, 073007 (2016).
[51] C. Jarzynski, Stochastic and Macroscopic Thermodynamics of Strongly Coupled Systems, Phys. Rev. X **7**, 011008 (2017).
[52] H. J. D. Miller, Hamiltonian of mean force for strongly-coupled systems, in *Thermodynamics in the Quantum Regime: Fundamental Aspects and New Directions* (Springer International Publishing, Cham, 2018), pp. 531–549, 10.1007/978-3-319-99046-0_22.
[53] M. Perarnau-Llobet, H. Wilming, A. Riera, R. Gallego, and J. Eisert, Strong coupling corrections in quantum thermodynamics, Phys. Rev. Lett. **120**, 120602 (2018).
[54] P. Strasberg and M. Esposito, Non-Markovianity and negative entropy production rates, Phys. Rev. E **99**, 012120 (2019).
[55] Á. Rivas, Strong coupling thermodynamics of open quantum systems, Phys. Rev. Lett. **124**, 160601 (2020).
[56] P. Strasberg, Thermodynamics of quantum causal models: An inclusive, Hamiltonian approach, Quantum **4**, 240 (2020).
[57] Y.-Y. Xu, J. Gong, and W.-M. Liu, Quantum thermodynamics with strong system-bath coupling: A mapping approach, arXiv:2304.08268.
[58] Z. Davoudi *et al.*, Quantum work and heat exchanged during sudden quenches of strongly coupled systems (to be published).
[59] Á. Rivas, Quantum thermodynamics in the refined weak coupling limit, Entropy **21**, 725 (2019).
[60] M. Campisi, P. Talkner, and P. Hänggi, Thermodynamics and fluctuation theorems for a strongly coupled open quantum system: An exactly solvable case, J. Phys. A **42**, 392002 (2009).
[61] P.V. Buividovich and M.I. Polikarpov, Entanglement entropy in gauge theories and the holographic principle for electric strings, Phys. Lett. B **670**, 141 (2008).
[62] W. Donnelly, Decomposition of entanglement entropy in lattice gauge theory, Phys. Rev. D **85**, 085004 (2012).
[63] H. Casini, M. Huerta, and J. A. Rosabal, Remarks on entanglement entropy for gauge fields, Phys. Rev. D **89**, 085012 (2014).
[64] D. Radicevic, Notes on entanglement in abelian gauge theories, arXiv:1404.1391.
[65] S. Aoki *et al.*, On the definition of entanglement entropy in lattice gauge theories, J. High Energy Phys. 06 (2015) 187.
[66] R. M. Soni and S. P. Trivedi, Aspects of entanglement entropy for gauge theories, J. High Energy Phys. 01 (2016) 136.
[67] K. Van Acoleyen, N. Bultinck, J. Haegeman, M. Marien, V. B. Scholz, and F. Verstraete, Entanglement of distillation for lattice gauge theories, Phys. Rev. Lett. **117**, 131602 (2016).
[68] A. Bulgarelli and M. Panero, Duality transformations and the entanglement entropy of gauge theories, J. High Energy Phys. 06 (2024) 041.
[69] A. Mitra, Quantum quench dynamics, Annu. Rev. Condens. Matter Phys. **9**, 245 (2018).
[70] E. Altman *et al.*, Quantum simulators: Architectures and opportunities, PRX Quantum **2**, 017003 (2021).
[71] A. J. Daley, I. Bloch, C. Kokail, S. Flannigan, N. Pearson, M. Troyer, and P. Zoller, Practical quantum advantage in quantum simulation, Nature (London) **607**, 667 (2022).
[72] Relationships between work distributions and phase transitions were explored recently in the context of spin systems [73–80].
[73] F.-L. Lin and C.-Y. Huang, Work statistics for quantum spin chains: Characterizing quantum phase transitions,

benchmarking time evolution, and examining passivity of quantum states, Phys. Rev. Res. **6**, 023169 (2024).
[74] A. Kiely, E. O'Connor, T. Fogarty, G. T. Landi, and S. Campbell, Entropy of the quantum work distribution, Phys. Rev. Res. **5**, L022010 (2023).
[75] H. Zhang, Y. Qian, Z.-X. Niu, and Q. Wang, Excited-stated quantum phase transitions and the entropy of the work distribution in the anharmonic Lipkin-Meshkov-Glick model, Phys. Rev. E **109**, 064110 (2024).
[76] K. Zawadzki, R. M. Serra, and I. D'Amico, Work-distribution quantumness and irreversibility when crossing a quantum phase transition in finite time, Phys. Rev. Res. **2**, 033167 (2020).
[77] Q. Wang and H. T. Quan, Probing the excited-state quantum phase transition through statistics of Loschmidt echo and quantum work, Phys. Rev. E **96**, 032142 (2017).
[78] E. Mascarenhas *et al.*, Work and quantum phase transitions: Quantum latency, Phys. Rev. E **89**, 062103 (2014).
[79] Z. Mzaouali, R. Puebla, J. Goold, M. El Baz, and S. Campbell, Work statistics and symmetry breaking in an excited-state quantum phase transition, Phys. Rev. E **103**, 032145 (2021).
[80] Z. Fei, N. Freitas, V. Cavina, H. T. Quan, and M. Esposito, Work statistics across a quantum phase transition, Phys. Rev. Lett. **124**, 170603 (2020).
[81] H. Li and F. D. M. Haldane, Entanglement spectrum as a generalization of entanglement entropy: Identification of topological order in non-Abelian fractional quantum Hall effect states, Phys. Rev. Lett. **101**, 010504 (2008).
[82] M. Dalmonte, V. Eisler, M. Falconi, and B. Vermersch, Entanglement Hamiltonians: From field theory to lattice models and experiments, Ann. Phys. (Berlin) **534**, 2200064 (2022).
[83] C. Kokail, R. van Bijnen, A. Elben, B. Vermersch, and P. Zoller, Entanglement Hamiltonian tomography in quantum simulation, Nat. Phys. **17**, 936 (2021).
[84] C. Kokail, B. Sundar, T. V. Zache, A. Elben, B. Vermersch, M. Dalmonte, R. van Bijnen, and P. Zoller, Quantum variational learning of the entanglement Hamiltonian, Phys. Rev. Lett. **127**, 170501 (2021).
[85] M. K. Joshi *et al.*, Exploring large-scale entanglement in quantum simulation, Nature (London) **624**, 539 (2023).
[86] N. Mueller, J. A. Carolan, A. Connelly, Z. Davoudi, E. F. Dumitrescu, and K. Yeter-Aydeniz, Quantum computation of dynamical quantum phase transitions and entanglement tomography in a lattice gauge theory, PRX Quantum **4**, 030323 (2023).
[87] C. Jarzynski, Nonequilibrium work theorem for a system strongly coupled to a thermal environment, J. Stat. Mech. (2004) P09005.
[88] P. Talkner and P. Hänggi, Colloquium: Statistical mechanics and thermodynamics at strong coupling: Quantum and classical, Rev. Mod. Phys. **92**, 041002 (2020).
[89] Boltzmann's constant is set to 1 throughout the Letter.
[90] J. Eisert, M. Friesdorf, and C. Gogolin, Quantum many-body systems out of equilibrium, Nat. Phys. **11**, 124 (2015).
[91] H. Bernien *et al.*, Probing many-body dynamics on a 51-atom quantum simulator, Nature (London) **551**, 579 (2017).
[92] J. Zhang, G. Pagano, P. W. Hess, A. Kyprianidis, P. Becker, H. Kaplan, A. V. Gorshkov, Z.-X. Gong, and C. Monroe, Observation of a many-body dynamical phase transition with a 53-qubit quantum simulator, Nature (London) **551**, 601 (2017).
[93] W. L. Tan *et al.*, Domain-wall confinement and dynamics in a quantum simulator, Nat. Phys. **17**, 742 (2021).
[94] S. Ebadi *et al.*, Quantum phases of matter on a 256-atom programmable quantum simulator, Nature (London) **595**, 227 (2021).
[95] A. De *et al.*, Non-equilibrium critical scaling and universality in a quantum simulator, arXiv:2309.10856.
[96] E. A. Martinez *et al.*, Real-time dynamics of lattice gauge theories with a few-qubit quantum computer, Nature (London) **534**, 516 (2016).
[97] N. Klco, E. F. Dumitrescu, A. J. McCaskey, T. D. Morris, R. C. Pooser, M. Sanz, E. Solano, P. Lougovski, and M. J. Savage, Quantum-classical computation of Schwinger model dynamics using quantum computers, Phys. Rev. A **98**, 032331 (2018).
[98] N. H. Nguyen, M. C. Tran, Y. Zhu, A. M. Green, C. Huerta Alderete, Z. Davoudi, and N. M. Linke, Digital quantum simulation of the Schwinger model and symmetry protection with trapped ions, PRX Quantum **3**, 020324 (2022).
[99] D. E. Kharzeev and Y. Kikuchi, Real-time chiral dynamics from a digital quantum simulation, Phys. Rev. Res. **2**, 023342 (2020).
[100] Z.-Y. Zhou, G.-X. Su, J. C. Halimeh, R. Ott, H. Sun, P. Hauke, B. Yang, Z.-S. Yuan, J. Berges, and J.-W. Pan, Thermalization dynamics of a gauge theory on a quantum simulator, Science **377**, 311 (2022).
[101] A. Elben, B. Vermersch, C. F. Roos, and P. Zoller, Statistical correlations between locally randomized measurements: A toolbox for probing entanglement in many-body quantum states, Phys. Rev. A **99**, 052323 (2019).
[102] H.-Y. Huang, R. Kueng, and J. Preskill, Predicting many properties of a quantum system from very few measurements, Nat. Phys. **16**, 1050 (2020).
[103] H.-Y. Huang *et al.*, Quantum advantage in learning from experiments, Science **376**, 1182 (2022).
[104] A. Elben *et al.*, The randomized measurement toolbox, Nat. Rev. Phys. **5**, 9 (2023).
[105] H. Pichler, G. Zhu, A. Seif, P. Zoller, and M. Hafezi, Measurement Protocol for the Entanglement Spectrum of Cold Atoms, Phys. Rev. X **6**, 041033 (2016).
[106] M. Dalmonte, B. Vermersch, and P. Zoller, Quantum simulation and spectroscopy of entanglement Hamiltonians, Nat. Phys. **14**, 827 (2018).
[107] J. Bringewatt, J. Kunjummen, and N. Mueller, Randomized measurement protocols for lattice gauge theories, Quantum **8**, 1300 (2024).
[108] N. Mueller, Unpublished notes, 2024.
[109] K. Matsumoto, Y. Shingu, S. Endo, S. Kawabata, S. Watabe, T. Nikuni, H. Hakoshima, and Y. Matsuzaki, Calculation of Gibbs partition function with imaginary

time evolution on near-term quantum computers, Jpn. J. Appl. Phys. **61**, 042002 (2022).
[110] Y. Wu and J. B. Wang, Estimating Gibbs partition function with quantum Clifford sampling, Quantum Sci. Technol. **7**, 025006 (2022).
[111] S. Arunachalam, V. Havlicek, G. Nannicini, K. Temme, and P. Wocjan, Simpler (classical) and faster (quantum) algorithms for Gibbs partition functions, Quantum **6**, 789 (2022).
[112] S. Bravyi, A. Chowdhury, D. Gosset, and P. Wocjan, Quantum Hamiltonian complexity in thermal equilibrium, Nat. Phys. **18**, 1367 (2022).
[113] R. Kawai, J. M. R. Parrondo, and C. Van den Broeck, Dissipation: The phase-space perspective, Phys. Rev. Lett. **98**, 080602 (2007).
[114] C. Jarzynski, Equalities and inequalities: Irreversibility and the second law of thermodynamics at the nanoscale, Annu. Rev. Condens. Matter Phys. **2**, 329 (2011).
[115] In the standard model of particle physics, nature sets the value of g.
[116] J. R. Stryker, Oracles for Gauss's law on digital quantum computers, Phys. Rev. A **99**, 042301 (2019).
[117] I. Raychowdhury and J. R. Stryker, Solving Gauss's law on digital quantum computers with loop-string-hadron digitization, Phys. Rev. Res. **2**, 033039 (2020).
[118] E. Zohar and B. Reznik, Confinement and lattice quantum-electrodynamic electric flux tubes simulated with ultracold atoms, Phys. Rev. Lett. **107**, 275301 (2011).
[119] D. Banerjee, M. Dalmonte, M. Müller, E. Rico, P. Stebler, U.-J. Wiese, and P. Zoller, Atomic quantum simulation of dynamical gauge fields coupled to fermionic matter: From string breaking to evolution after a quench, Phys. Rev. Lett. **109**, 175302 (2012).
[120] E. Zohar, J. I. Cirac, and B. Reznik, Simulating $(2+1)$-dimensional lattice QED with dynamical matter using ultracold atoms, Phys. Rev. Lett. **110**, 055302 (2013).
[121] L. Tagliacozzo, A. Celi, P. Orland, M. W. Mitchell, and M. Lewenstein, Simulation of non-abelian gauge theories with optical lattices, Nat. Commun. **4**, 2615 (2013).
[122] P. Hauke, D. Marcos, M. Dalmonte, and P. Zoller, Quantum Simulation of a Lattice Schwinger Model in a Chain of Trapped Ions, Phys. Rev. X **3**, 041018 (2013).
[123] Z. Davoudi, N. Mueller, and C. Powers, Towards quantum computing phase diagrams of gauge theories with thermal pure quantum states, Phys. Rev. Lett. **131**, 081901 (2023).
[124] J. C. Halimeh, H. Lang, J. Mildenberger, Z. Jiang, and P. Hauke, Gauge-symmetry protection using single-body terms, PRX Quantum **2**, 040311 (2021).
[125] J. C. Halimeh and P. Hauke, Stabilizing Gauge Theories in Quantum Simulators: A Brief Review, arXiv:2204.13709.
[126] See Supplemental Material at http://link.aps.org/supplemental/10.1103/PhysRevLett.133.250402, which includes Ref. [127], for discussions regarding numerical stability of results and the use of weak-coupling approximations in calculating thermodynamic quantities for the LGT system described in the main text.
[127] C. De Sa, Low-precision arithmetic, CS4787 Lecture 21, Cornell University (2020).
[128] For a pure gauge theory, which lacks matter fields, the operator reduces to $G_n \coloneqq \tilde{\sigma}^x_n \tilde{\sigma}^x_{n-1}$. This is the familiar generator of a local $\mathbb{Z}_2$ symmetry.
[129] Numerical computations of this work are performed by manually restricting to the physical Hilbert space.
[130] Σ has the form that the chiral condensate would have if the gauge field were coupled to staggered fermions [11] (a Jordan-Wigner transformation maps the fermion operators to Pauli operators). Such a chiral condensate serves as an order parameter for chiral phase transitions.
[131] We have not performed a large-system analysis to confirm if the apparent phase transition persists in the thermodynamic limit. However, large-system analyses of a similar model (with the same discrete chiral symmetry as ours) reveal two phases, confined and deconfined [132,133]. While these studies do not directly probe the spontaneous breaking of the discrete chiral symmetry, the symmetry is broken in the confined phase.
[132] M. Kebrič, L. Barbiero, C. Reinmoser, U. Schollwöck, and F. Grusdt, Confinement and Mott transitions of dynamical charges in one-dimensional lattice gauge theories, Phys. Rev. Lett. **127**, 167203 (2021).
[133] M. Kebrič, J. C. Halimeh, U. Schollwöck, and F. Grusdt, Confinement in $(1+1)$-dimensional $\mathbb{Z}_2$lattice gauge theories at finite temperature, Phys. Rev. B **109**, 245110 (2024).
[134] X.-G. Wen, Topological orders in rigid states, Int. J. Mod. Phys. B **04**, 239 (1990).
[135] A.Yu. Kitaev, Fault-tolerant quantum computation by anyons, Ann. Phys. (Amsterdam) **303**, 2 (2003).
[136] M. A. Levin and X.-G. Wen, String-net condensation: A physical mechanism for topological phases, Phys. Rev. B **71**, 045110 (2005).
[137] B. A. Bernevig (with T. L. Hughes) *Topological Insulators and Topological Superconductors* (Princeton University Press, Princeton, NJ, 2013).
[138] K. Seo, C. Zhang, and S. Tewari, Thermodynamic signatures for topological phase transitions to Majorana and Weyl superfluids in ultracold Fermi gases, Phys. Rev. A **87**, 063618 (2013).
[139] S. N. Kempkes, A. Quelle, and C. Morais Smith, Universalities of thermodynamic signatures in topological phases, Sci. Rep. **6**, 38530 (2016).
[140] D. Caputo *et al.*, Topological order and thermal equilibrium in polariton condensates, Nat. Mater. **17**, 145 (2018).
[141] A. Carollo, D. Valenti, and B. Spagnolo, Geometry of quantum phase transitions, Phys. Rep. **838**, 1 (2020).
[142] M. Heyl, Dynamical quantum phase transitions: A review, Rep. Prog. Phys. **81**, 054001 (2018).
[143] C. Schweizer, F. Grusdt, M. Berngruber, L. Barbiero, E. Demler, N. Goldman, I. Bloch, and M. Aidelsburger, Floquet approach to $\mathbb{Z}_2$ lattice gauge theories with ultracold atoms in optical lattices, Nat. Phys. **15**, 1168 (2019).
[144] B. Yang, H. Sun, R. Ott, H.-Y. Wang, T. V. Zache, J. C. Halimeh, Z.-S. Yuan, P. Hauke, and J.-W. Pan, Observation of gauge invariance in a 71-site Bose–Hubbard quantum simulator, Nature (London) **587**, 392 (2020).

[145] S. Notarnicola, M. Collura, and S. Montangero, Real-time-dynamics quantum simulation of $(1+1)$-dimensional lattice QED with Rydberg atoms, Phys. Rev. Res. **2**, 013288 (2020).
[146] F. M. Surace, P. P. Mazza, G. Giudici, A. Lerose, A. Gambassi, and M. Dalmonte, Lattice gauge theories and string dynamics in Rydberg atom quantum simulators, Phys. Rev. X **10**, 021041 (2020).
[147] N. Klco, M. J. Savage, and J. R. Stryker, SU(2) non-Abelian gauge field theory in one dimension on digital quantum computers, Phys. Rev. D **101**, 074512 (2020).
[148] A. Ciavarella, N. Klco, and M. J. Savage, Trailhead for quantum simulation of SU(3) Yang-Mills lattice gauge theory in the local multiplet basis, Phys. Rev. D **103**, 094501 (2021).
[149] W. A. de Jong *et al.*, Quantum simulation of nonequilibrium dynamics and thermalization in the Schwinger model, Phys. Rev. D **106**, 054508 (2022).
[150] J. Mildenberger, W. Mruczkiewicz, J. C. Halimeh, Z. Jiang, and P. Hauke, Probing confinement in a $\mathbb{Z}_2$ lattice gauge theory on a quantum computer, arXiv:2203.08905.
[151] J. C. Halimeh, I. P. McCulloch, B. Yang, and P. Hauke, Tuning the topological θ-angle in cold-atom quantum simulators of gauge theories, PRX Quantum **3**, 040316 (2022).
[152] W.-Y. Zhang *et al.*, Observation of microscopic confinement dynamics by a tunable topological θ-angle, arXiv:2306.11794.
[153] C. Charles, E. J. Gustafson, E. Hardt, F. Herren, N. Hogan, H. Lamm, S. Starecheski, R. S. Van de Water, and M. L. Wagman, Simulating $\mathbb{Z}_2$ lattice gauge theory on a quantum computer, Phys. Rev. E **109**, 015307 (2024).
[154] F. M. Surace and A. Lerose, Scattering of mesons in quantum simulators, New J. Phys. **23**, 062001 (2021).
[155] R. Belyansky, S. Whitsitt, N. Mueller, A. Fahimniya, E. R. Bennewitz, Z. Davoudi, and A. V. Gorshkov, High-energy collision of quarks and mesons in the Schwinger model: From tensor networks to circuit QED, Phys. Rev. Lett. **132**, 091903 (2024).
[156] Y. Chai *et al.*, Fermionic wave packet scattering: A quantum computing approach, arXiv:2312.02272.
[157] G.-X. Su, J. Osborne, and J. C. Halimeh, A cold-atom particle collider, arXiv:2401.05489.
[158] R. C. Farrell, M. Illa, A. N. Ciavarella, and M. J. Savage, Quantum Simulations of Hadron Dynamics in the Schwinger Model using 112 Qubits, Phys. Rev. D **109**, 114510 (2024).
[159] Z. Davoudi, C.-C. Hsieh, and S. V. Kadam, Scattering wave packets of hadrons in gauge theories: Preparation on a quantum computer, arXiv:2402.00840.